



ELSEVIER

Journal of Non-Crystalline Solids 307–310 (2002) 913–920

JOURNAL OF  
NON-CRYSTALLINE SOLIDS

www.elsevier.com/locate/jnoncrystal

# Discrimination between series and parallel fitting models for nearly constant loss effects in dispersive ionic conductors

J. Ross Macdonald \*

*Department of Physics and Astronomy, University of North Carolina, Chapel Hill, NC 27599-3255, USA*

## Abstract

The important effects of electrode polarization on the conductivity of ionic materials are illustrated for both low- and high-frequency regions. Experimental data fitting and simulation with a fully complex model, including a part representing ionic dispersion and constant-phase-element (CPE) power-laws in series or in parallel, show that the series element, usually representing electrode effects, can lead to  $\sigma'(\omega)$  log–log slopes of 1.3 or more. In addition, over a substantial frequency region, such effects can yield  $\sigma(\omega)$  response indistinguishable from that following from the parallel combination of the ionic dispersion model, here a form of Kohlrausch–Williams–Watts behavior, and a CPE. With a sufficiently wide experimental frequency range, one can discriminate between these two possibilities and identify the one that is associated with the measured experimental behavior. The problem of discrimination is particularly difficult, however, for low-temperature data that show nearly-constant-loss  $\varepsilon''(\omega)$  response. In contrast to recent conclusions, such response can be modeled and well fitted with a composite model involving either a series or a parallel CPE.

© 2002 Elsevier Science B.V. All rights reserved.

PACS: 72.20.-i; 66.10.Ed; 77.22.Gm; 81.05.Kf

## 1. Introduction and background

In the past, electrode effects in immittance spectroscopy data have often been unmentioned, unrecognized, characterized as unimportant, and/or ignored [1–6]. A frequently used argument is that presentation of data at the electric modulus level, (where  $M(\omega) = M'(\omega) + iM''(\omega) = 1/\varepsilon(\omega) = i\omega\varepsilon_V\rho(\omega)$ ) makes any electrode effects present negligible in  $M''(\omega)$ . Here  $\varepsilon(\omega) = \varepsilon'(\omega) - i\varepsilon''(\omega)$  is

the complex dielectric constant;  $\rho(\omega) = 1/\sigma(\omega)$  is the complex resistivity;  $\sigma(\omega)$  is the complex conductivity; and  $\varepsilon_V$  is the permittivity of vacuum. On the other hand, some treatments of low-frequency electrode effects have appeared (see for example, Refs. [7–9]).

While it is true that low-frequency electrode effects are reduced by a factor of  $\omega$  in an  $M''(\omega)$  plot, as compared to a  $\rho'(\omega)$  plot, they are, of course, still fully present in the data, and proportional-weighting complex non-linear least squares (CNLS) fitting [10] of the same data expressed at either the  $M(\omega)$  or the  $\rho(\omega)$  level leads to exactly the same parameter estimates. Thus, if the model

\* Tel.: +1-919 967 5005; fax: +1-919 962 0480.

E-mail address: [macd@email.unc.edu](mailto:macd@email.unc.edu) (J.R. Macdonald).

includes parameters representing electrode polarization contributions, they will be identically estimated by fits at either level.

Another frequent misconception is that because one fitting model has fewer parameters than another, the former is preferable to the latter [3]. This type of thinking, not based on detailed CNLS fitting of the data, has led, for example, to the widespread use of the original three-parameter modulus formalism (OMF), rather than a model with more parameters. (see for example, the 20 references to the OMF in Ref. [11]). But crucial defects in the OMF model have been pointed out since 1996 and a corrected version, the CMF, proposed and its usefulness illustrated [12–16]. In addition to the presence of a minimal number of free parameters in the OMF, another of its apparent virtues and one of the main reasons for its endemic use is its fitting simplicity. Thus, the important shape parameter of the model,  $\beta = \beta_1$ , can be well estimated entirely from a graphical determination of the full width at half height of an experimental  $M''(\omega)$  curve [17].

Unfortunately, as shown by fitting with the four-parameter CMF model, OMF parameter estimates of  $\tau_0$ , the characteristic relaxation time of the fitting model (a form of Kohlrausch–Williams–Watts (KWW) response [18], the KWW1) and its  $\beta_1$  shape parameter are not appropriate and significant [12–16,19,20]. This is because the OMF does not properly include the effects of the bulk dielectric constant of the material,  $\varepsilon_{D\infty}$  [12–16]. It follows that earlier conclusions about physical processes such as ion–ion correlation, based on variation of  $\beta_1$  with temperature or ion concentration, are usually misleading and inapplicable [19,20].

Further, the number of free parameters included in a fitting model is far less important than are the relative standard deviation of the fit,  $S_F$ , and the relative standard deviations of the individual free parameters for a given model. Clearly a poor fitting model with one or more non-significant parameter standard deviations should not be preferred to a more appropriate better fitting model with all of its parameter standard deviations highly significant, even when the latter involves more parameters than the former. The LEVM CNLS computer program [10] leads to fitting re-

sults that may be used in an included  $F$ -test statistical estimate of the probability that adding additional free fitting parameters to a model is warranted. This test, when applied for fits of many different materials, shows, statistically speaking, that the OMF is much less appropriate than the CMF. See Refs. [13–16,20] for other facts supporting this conclusion.

Both the OMF and the CMF models use the conductive-system KWW dispersion model, the KWW1, here abbreviated as the K1 [16]. Although the frequency response of the K1 cannot be expressed in closed form for arbitrary  $\beta_1$  values, the LEVM program allows one to calculate such response to an accuracy usually better than one part in  $10^5$  and thus to simulate or fit data accurately. Contrary to earlier statements or implications, K1 frequency response is not a direct Fourier transform of stretched-exponential temporal response [13,14,19,21]. Unlike most other response models, the K1 leads to a non-zero high-frequency-limiting value of  $\varepsilon_C(\omega)$ ,  $\varepsilon_{C1\infty}$ , where the subscript ‘C’ indicates conductive-system response.

The CMF includes a separate free  $\varepsilon_{D\infty}$  parameter in parallel with the K1 ion-only response, and is designated the CK1 model. In addition, in the present work the following composite models will be used or discussed, the CK1S, the PK1, and the PK1S. Here, the S symbol stands for SCPE response, a constant-phase-angle element [22,23] in series with the rest of the response and represented by  $\sigma_{SC}(\omega) = \varepsilon_V A_{SC}(i\omega)^{\gamma_{SC}}$  with  $0 \leq \gamma_{SC} \leq 1$ . The P symbol stands for PCPE response, a constant-phase-angle element in parallel with the K1 dispersion model. It is expressed as  $\sigma_{PC}(\omega) = \varepsilon_V A_{PC}(i\omega)^{1-\gamma_{PC}}$  with  $0 \leq \gamma_{PC} \leq 1$ . Note that when  $\gamma_{SC} = 1$  the SCPE leads to complete blocking of mobile charges at the electrodes. When  $\gamma_{PC} = 0$  the  $A_{PC}$  element of the PCPE represents a frequency-independent dielectric constant and the PK1 model reduces to the CK1 one. Thus, when  $\gamma_{PC} \ll 1$ , we can set  $A_{PC} \simeq \varepsilon_{D\infty}$ . For this condition, or when  $0 < 1 - \gamma_{SC} \ll 1$ , the response will include  $\varepsilon''(\omega)$  power-law response with a very small exponent: nearly constant loss (NCL) behavior [23].

In a recent analysis of data involving variable ionic concentration [20], it has been demonstrated that the assumption of a frequency-independent

$\varepsilon_{D\infty}$  parameter is apparently only entirely appropriate in the limit of zero ionic concentration. For non-zero concentrations, accurate fitting requires that in addition to the zero-concentration value of  $\varepsilon_{D\infty}$ , denoted  $\varepsilon_{D\infty 0}$ , a small, complex, frequency-dependent term must be added, well represented by the PCPE element with  $\gamma_{PC} \ll 0$  and with  $A_{PC}$  increasing as the concentration increases. These results imply that this NCL increase in the effective bulk dielectric constant associated with dipolar and vibratory effects of the network material arises from interaction with mobile charges, particularly at high frequencies where ions are localized and librate [20].

Finally, it should be mentioned that Nowick et al. [9] and others have shown that considerable conductive-system data may be fitted with a composite model that may be expressed as

$$\sigma'(\omega) = \sigma_0[1 + (\omega/\omega_0)^n] + A\omega^m, \quad (1)$$

with  $0 < n \leq 1$ ,  $m \approx 1$  and  $\sigma'(0) \equiv \sigma_0$ . Here the  $A\omega^m$  term with  $1 - m \ll 1$  and positive represents the real part of NCL response. The first expression on the right models mobile-charge dispersion effects and has been called universal dynamic response [9,14]. Although Eq. (1) fits of  $\sigma'(\omega)$  data have usually led to  $0.6 \leq n \leq 0.7$  values and to  $m \simeq 1$ , they can only be trusted to involve NCL when electrode effects are either negligible in the measurement range or are separately accounted for, as in the PK1S model. Otherwise, the  $A\omega^m$  term may unwittingly represent electrode effects rather than NCL ones. See further discussion of this matter in Section 3. Note that CMF fits with either the CK1S or PK1S model lead to estimates of the high-frequency-limiting slope associated only with K1 of  $(1 - \beta_1) \simeq 2/3$ . Such values have been shown to be virtually independent of both temperature and ion concentration [16,19,20].

The PK1S model is a generalization and improvement on that of Eq. (1) in several respects. First, it is fully complex and its real and imaginary parts satisfy the Kronig–Kramers relations. Second, the K1 model has been found to be more appropriate for conductive-system data fitting than the complex version of the first term on the right of Eq. (1), the ZC model [14,22]. One reason is that, unlike the K1, the ZC involves a non-

physical low-frequency limiting slope. Finally, the inclusion of SCPE response allows the importance of electrode effects to be evaluated, and, when they are significant in the measured frequency range, it leads to their quantification and to better fits. In this case, fitting yields a clear distinction between the K1 limiting slope  $(1 - \beta_1)$  and electrode-effect slopes associated with  $\gamma_{SC}$ .

It should be mentioned that constant-phase-element (CPE) response elements have been included as parts of a full fitting model in the present work because of their simplicity and fitting utility, not because their forms are expected to apply exactly over the full frequency range from zero to infinity. At the extremes of frequency their forms must change to satisfy physical realizability, but actual data do not usually extend to such extremes. Nevertheless, CPE elements provide a good first approximation to fractal and other more complicated electrode-related responses. In the following, first low- and high-frequency electrode effects are illustrated for wide frequency ranges and CK1S fitting carried out. Then, comparisons are made between fitting CK1S synthetic data with a PK1 model and vice versa in order to suggest how one can discriminate between the effects of a CPE in parallel with an ionic dispersion model and a CPE in series with it.

## 2. Data and electrode-effects fitting and analysis

Fig. 1 shows wide-temperature-range  $0.88\text{ZrO}_2 \cdot 0.12\text{Y}_2\text{O}_3$   $\sigma'(\omega)$  data [4], kindly supplied by Dr C. León. We see that the data become irregular at the lowest frequencies and temperatures and show different behavior at low temperatures than at high ones. Interesting details of the response appear in the Fig. 2 plot of the slopes of the log–log curves of Fig. 1. Particularly significant are slope values exceeding unity for the three lower temperatures. Also notice the abrupt change at about 67 kHz in the slopes of the lower-temperature curves.

It is clear that much of the data shown in Figs. 1 and 2 are entirely inconsistent with models such as those recently summarized by Dyre and Schrøder [24] and Funke [25,26]. These models lead, in the absence of a high-frequency plateau in  $\sigma'(\omega)$ , to

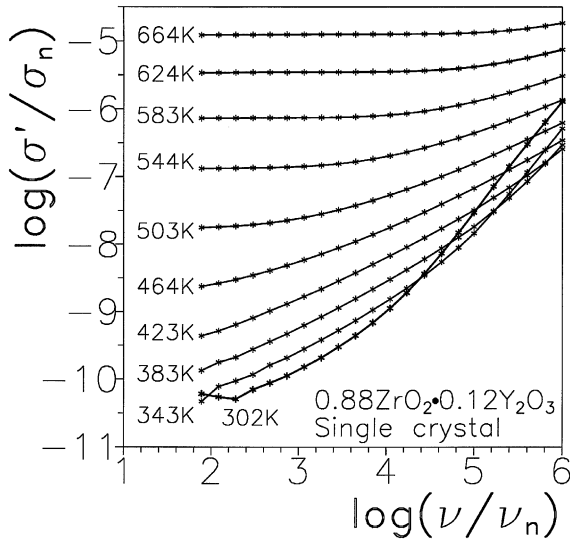


Fig. 1. Log–log plots of  $0.88\text{ZrO}_2 \cdot 0.12\text{Y}_2\text{O}_3$   $\sigma'(\omega)$  data for a range of temperatures. The quantity  $\sigma_n = 1$  mho/cm and  $\nu_n = 1$  Hz.

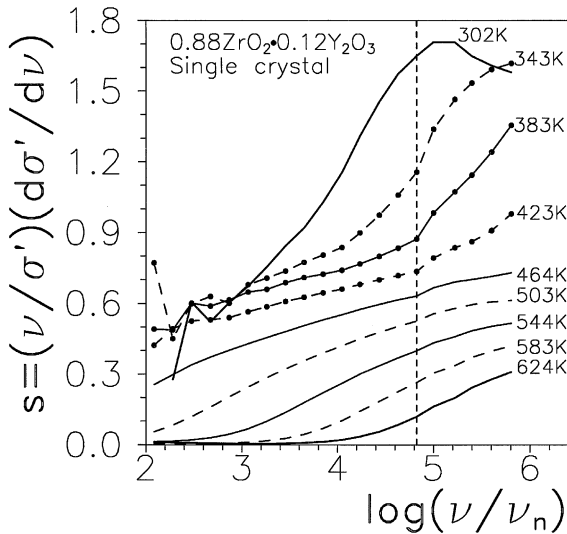


Fig. 2. Slopes of the  $\sigma'(\omega)$  lines of Fig. 1.

slopes monotonically increasing toward a unity asymptote. Incidentally, unpublished work of the author shows that the DCA symmetric-hopping dispersion model [24] may be exceptionally well fitted over eight or more decades of  $\sigma'(\omega)$  using a PK1 model, quite different in form from the Dyre and Schröder model. In addition, unlike the DCA

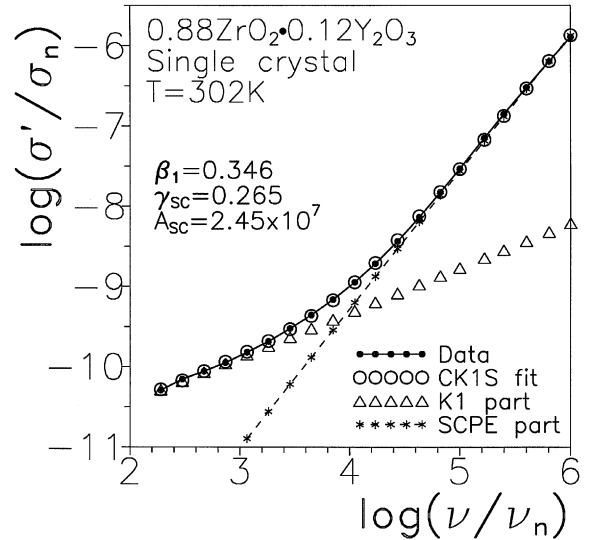


Fig. 3. CK1S fit of the 302 K data of Fig. 1. The fit involved only three free parameters: two SCPE ones and  $\varepsilon_{D\infty}$ .

model, the PK1 leads to physically plausible low-frequency-limiting slopes of the quantities  $(\sigma'(\omega) - \sigma_0)$  and  $\sigma''(\omega)$ .

Fig. 3 shows a CK1S fit of the present 302 K data with a few very irregular low-frequency points omitted and with fixed values of the three K1 parameters extrapolated from higher temperature fits [20]. The figure also includes the separate K1 and SCPE contributions to the full fit and thus shows low- and high-frequency limiting slopes. It is clear that the full model fits the data very well and that the SCPE, here modeling electrode effects, dominates the response at high frequencies. In previous work [23], it has been shown that the series combination of an ideal capacitance and a CPE can lead to  $\sigma'(\omega)$  response with a slope of  $(2 - \gamma_{SC})$  over an appreciable frequency range. Here the effective ideal capacitance at high frequencies is that associated with  $\varepsilon_{\infty} = \varepsilon_{Cl\infty} + \varepsilon_{D\infty}$ , thus arising from both ionic motion and dipolar/vibratory contributions of the bulk material.

These results show that electrode effects can be dominant at high frequencies, although they are usually thought to be important only at low frequencies [7–9]. It is thus of interest to show wide-range simulated data calculated with the CK1S model using the parameter values estimated from

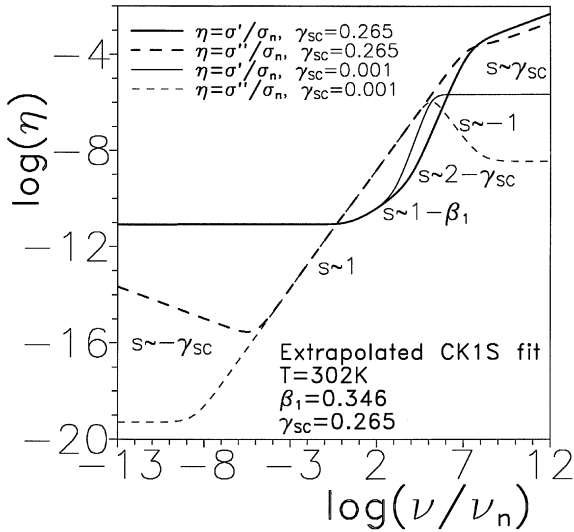


Fig. 4. Log-log plots of  $\sigma(\omega)$  model response calculated by extrapolation of the CK1S-fit results of Fig. 3.

the Fig. 3 fit. Such results, along with approximate slope values, are shown in Fig. 4 for the very large range of 25 decades. As the temperature decreases, an experimental frequency window of five or six decades will move to the left of the graph and beginning to show electrode-effect low-frequency deviations from CK1 response. Note that in addition to the results following from the Fig. 3 fit, ones with the very small  $\gamma_{sc}$  value of 0.001 are also included. Then the SCPE closely approximates a series resistance. For the present situation, it is evident that there is only a relatively small frequency range over which separate CK1 response is significant. Further, the high-frequency end of the data here is nearly high enough that the final high-frequency SCPE slope of  $\gamma_{sc}$  is apparent. Nevertheless, electrode-related slopes of  $(2 - \gamma_{sc}) \geq 1$  have frequently been evident in  $\sigma'(\omega)$  data.

Fig. 5 presents CK1S fitting results for the 624 K data of Fig. 1. For clarity, only every other fit value is included here. Note the different scales for  $\sigma'(\omega)$  and  $\sigma''(\omega)$ . Again, the fits are excellent and CK1S response dominates for  $\nu \geq 10^4$  Hz. For  $\nu \leq 10^3$ , on the other hand, SCPE ‘low-frequency’ contributions become evident. Note that the  $\beta_1$  values in Figs. 3 and 5 are the same, consistent with the  $\beta_1$  temperature independence found for

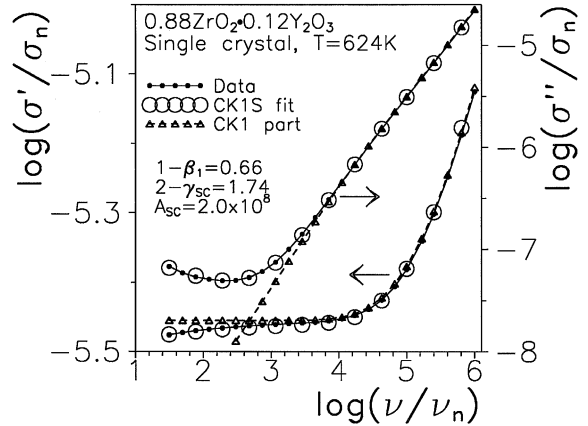


Fig. 5. CK1S fit of the 624 K data of Fig. 1. The fit involved six free parameters.

CK1 CMF fits at other temperatures for the present material [20].

Fig. 6 shows the wide-range extrapolation of the CK1S fit of Fig. 5. We see that although the same general behavior is apparent for both the 302 and 624 K extrapolations, the lower-frequency part of the  $\sigma''(\omega)$  curves of Fig. 6 appear roughly eight decades higher than those of Fig. 4 and the lower-frequency  $\sigma'(\omega)$  ones are at least four decades higher. The limiting very low-frequency  $\gamma_{sc}$

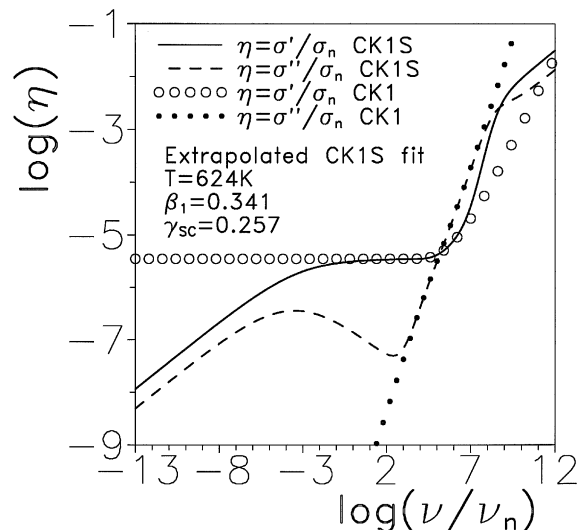


Fig. 6. Log-log plots of  $\sigma(\omega)$  model response calculated by extrapolation of the CK1S-fit results of Fig. 5.

slopes shown in Fig. 6 are rarely evident in actual data because insufficient low-frequency data are available. Nevertheless, Fig. 4 of Ref. [8], for  $\text{CaTiO}_3:30\%\text{Al}^{3+}$  data, presents a good fit of curves of exactly the same shape as those shown here below about  $10^8$  Hz,  $\sigma''(\omega)$  peak and all, and even Fig. 5 shows the beginning of the rise toward such a peak.

### 3. Discrimination between response models involving series or parallel elements

Here I consider the similarities and differences between NCL response associated with the CK1S and PK1 composite models, both instances of the corrected modulus formalism approach [12–16]. To do so, data sets were generated for a range of frequencies and temperatures using plausible parameter values for both models. Values were selected to be at least roughly appropriate for the response of tri-silicate glass presented in Figs. 7 and 9 of Ref. [9].

The K1 mobile-charge dispersion model leads to

$$\varepsilon_{C1\infty} = \sigma_0 \langle \tau \rangle_{01} / \varepsilon_V = \sigma_0 \tau_0 \Gamma(1/\beta_1) / \beta_1 \varepsilon_V \propto 1/T, \quad (2)$$

where  $\langle \tau \rangle_{01}$  is the mean of the K1 characteristic relaxation time,  $\tau_0$ , over the distribution of relaxation times associated with stretched-exponential response with shape parameter  $\beta_1$ , and  $\Gamma(\ )$  is the Euler gamma function. For the thermally activated  $\tau_0$ , we use  $\tau_0 = 8.355 \times 10^{-17} \exp(E/kT)$  with  $E = 0.71$  eV. In addition, we set  $\beta_1 = 0.35$  and  $\varepsilon_{D\infty} = 5$ , both independent of temperature. It then follows from Eq. (2) that  $\sigma_0 = \alpha/T\tau_0$ , and we use  $\alpha = 2.566 \times 10^{-11}$  with the units of  $\sigma_0$  taken as mho/cm. For this situation  $T\sigma_0$  involves the same activation energy as  $\tau_0$ . Data sets were constructed with values of  $\tau_0$  ranging from  $10^{-5}$  to  $10^7$  s in steps of 100. The corresponding temperatures varied from 323 K down to 155 K.

Fig. 7 presents CK1S data involving the SCPE parameter expressions shown on the graph. Here  $A_{SC}$  varied from about 186 to 1000 as the temperature increased. The 0.01 value in the exponent

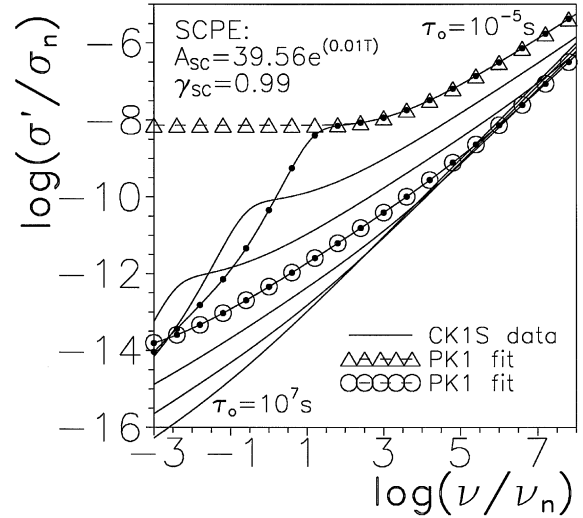


Fig. 7. Log-log plots of synthetic data generated using a series CK1S composite response model with two CNLS fits of such data using the parallel PK1 model.

of the  $A_{SC}$  exponential expression is of the order of magnitude of values found in Refs. [20,27]. In addition, Fig. 7 shows the results of PK1 CNLS fits of two CK1S data sets with all five PK1 parameters free to vary. It is evident that the PK1 cannot model the rapid low-frequency decrease in  $\sigma'(\omega)$  apparent in the top curve, but it turns out that it can fit the response at frequencies beyond this extremely well with values of  $\gamma_{PC} \leq 0.01$ , true NCL. Note that the present modeling results show the same crossover of curves present in the data of Fig. 1 at low temperatures and high frequencies. But there the maximum slope was of the order of 1.7, while here it does not quite reach unity.

It is the bottom four of the curves in Fig. 7 that approach NCL behavior at their higher-frequency ends, and it is response of this type which can alternatively be excellently fitted with the PK1 model. Although even CNLS fitting will not allow clear discrimination between the present series and parallel models for such data, it is evident that if the temperature is raised enough, or if the frequency range is extended to sufficiently low values, such discrimination will become possible.

Fig. 8 starts with the same K1 values as those used to obtain the results of Fig. 7, but synthetic

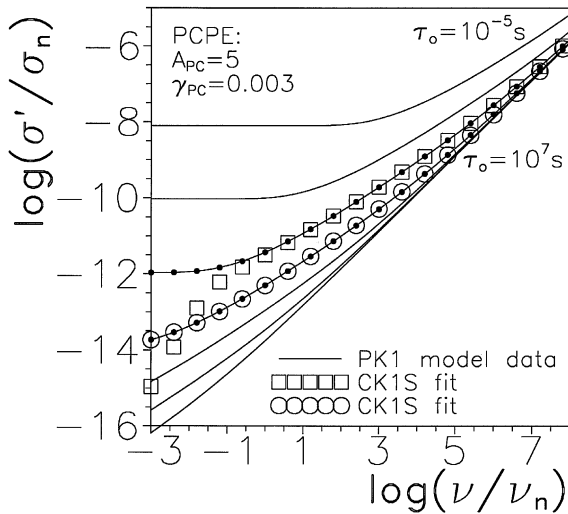


Fig. 8. Log-log plots of synthetic data generated using a parallel PK1 composite response model with two CNLS fits of such data using the series CK1S model.

data were here calculated with the PK1 parallel model using the fixed PCPE parameter values shown on the graph. Unlike the CK1S curves, the PK1 ones do not lead to a crossover at high frequencies, and the general shape and spacing of the PK1 lines are quite similar to those shown in Fig. 9 of Ref. [9]. The two CK1S six-parameter CNLS fit results included in Fig. 8 are consistent with the fitting comparisons of Fig. 7 and demonstrate that the CK1S model can here fit PK1 complex data for the  $\tau_o \geq 10$  s responses. Earlier work has shown that a capacitance in series or in parallel with a CPE element (CP and CS models) can lead equivalently to a type of NCL response [23]; here more complicated composite response models are also shown to lead to NCL.

Even in situations where the CK1S and PK1 models can fit putative NCL data equally well, it may be plausible, in the absence of evident electrode polarization effects in the data, to chose the PK1 model rather than to assume that nearly, but not quite exact complete, blocking of the mobile charges at the electrodes is present. Nevertheless, for most experiments on disordered materials and glasses with non-parent-ion electrodes, it is reasonable to expect that electrode polarization with nearly complete blocking will be important in some

frequency-response regions, often those outside the experimentally measured frequency range. It is therefore wise to fit data with such a model as the PK1S and obtain estimates of PCPE and SCPE parameter uncertainties. Such fits often allow one to discriminate between the effects of these two elements and to identify the PCPE contribution with NCL behavior and the SCPE one with electrode polarization [20,23].

Finally, important recent  $\sigma'(\omega, T)$  results of León et al. [27] dealing with NCL effects, but not including CNLS fitting, led these authors to conclude that their data could not be explained by an additive (parallel) model such as that of Eq. (1). In contrast, the present results suggest that at least trisilicate data, such as that of Ref. [9], can indeed be explained over substantial frequency and temperature ranges (including those where NCL effects are evident) by a parallel or a series composite model, the PK1 or the CK1S. As discussed elsewhere [20,27], the work of Ref. [27] led to a physical model for ionic motion yielding NCL at odds with that following from detailed CNLS analysis of experimental data [20]. Future work should help decide the applicability of these two disparate NCL explanations and show whether data such as those considered in Ref. [27] can be properly explained by a series or by a parallel response model (or by either!).

## Acknowledgements

Part of this work was presented at the 4th International Discussion Meeting on Relaxations in Complex Systems, Crete, Greece, 18 June, 2001. It is a pleasure to thank Dr Carlos Leon for valuable discussions relevant to the present analysis and interpretations.

## References

- [1] R.H. Cole, E. Tombari, *J. Non-Cryst. Solids* 131–133 (1991) 969.
- [2] I. Svare, F. Borsa, D.R. Torgeson, S.W. Martin, H. Patel, *J. Non-Cryst. Solids* 185 (1995) 297.
- [3] C.T. Moynihan, *Solid State Ionics* 105 (1998) 175.

- [4] A. Pimenov, J. Ullrich, P. Lunkenheimer, A. Loidl, C.H. Ruscher, *Solid State Ionics* 109 (1998) 111.
- [5] D. Sidebottom, *Phys. Rev. Lett.* 82 (1999) 3653.
- [6] K.L. Ngai, C. León, *Solid State Ionics* 125 (1999) 81.
- [7] D.L. Sidebottom, P.F. Green, R.K. Brow, *J. Non-Cryst. Solids* 183 (1995) 151.
- [8] J.R. Macdonald, *J. Non-Cryst. Solids* 210 (1997) 70.
- [9] A.S. Nowick, A.V. Vaysleyb, W. Liu, *Solid State Ionics* 105 (1998) 121.
- [10] J.R. Macdonald, L.D. Potter Jr., *Solid State Ionics* 23 (1987) 61;  
J.R. Macdonald, *J. Comput. Phys.* 157 (2000) 280.  
The newest version of the comprehensive LEVM fitting program may be downloaded at no cost from <http://www.physics.unc.edu/~macd/>. It includes an extensive manual, executable programs, and full source code. More information is provided about LEVM at this www address.
- [11] K.L. Ngai, C. León, *Phys. Rev. B* 60 (1999) 9396.
- [12] J.R. Macdonald, *J. Non-Cryst. Solids* 197 (1996) 83;  
Erratum: *J. Non-Cryst. Solids* 204 (1996) 309. In addition,  $G_D$  in Eq. (A2) should be  $G_{CD}$ .
- [13] J.R. Macdonald, *J. Non-Cryst. Solids* 212 (1997) 95;  
Erratum: *J. Non-Cryst. Solids* 220 (1997) 107, Eq. (7) should only be applied when  $0 \leq \rho_{C_\infty} < \rho_{C_0}$ . Also, the symbol  $\sigma$  should be removed from the right end of Eq. (12) and 'dx' should be moved from the left side of the term in square brackets in Eq. (A5) to the right side.
- [14] J.R. Macdonald, *Solid State Ionics* 133 (2000) 79.
- [15] J.R. Macdonald, *Phys. Rev. B* 63 (2001) 052205.
- [16] J.R. Macdonald, *J. Appl. Phys.* 90 (2001) 153, In Eq. (10),  $\sigma_0 \Gamma$  should be replaced by  $\sigma_0 \tau_0 \Gamma$ .
- [17] C.T. Moynihan, L.P. Boesch, N.L. Laberge, *Phys. Chem. Glasses* 14 (1973) 122.
- [18] R. Kohlrausch, *Pogg. Ann. Phys. Chem.* 91 (2) (1854) 179;  
G. Williams, D.C. Watts, *Trans. Faraday Soc.* 66 (1970) 80.
- [19] J.R. Macdonald, *Solid State Ionics*, in press.
- [20] J.R. Macdonald, *J. Chem. Phys.* 116 (2002) 3401.
- [21] J.R. Macdonald, *J. Appl. Phys.* 84 (1998) 812.
- [22] J.R. Macdonald (Ed.), *Impedance Spectroscopy—Emphasizing Solid Materials and Systems*, Wiley-Interscience, New York, 1987.
- [23] J.R. Macdonald, *J. Chem. Phys.* 115 (2001) 6192.
- [24] J.C. Dyre, T.B. Schröder, *Rev. Mod. Phys.* 72 (2000) 873.
- [25] K. Funke, D. Wilmer, *Solid State Ionics* 136&137 (2000) 1329.
- [26] J.R. Macdonald, *Solid State Ionics* 124 (1999) 1.  
Erratum: the heading 'Appendix' was omitted in page setting and should have been included on p. 18 after the third line of the Acknowledgments Section.
- [27] C. León, A. Rivera, A. Várez, J. Sanz, J. Santamaria, K.L. Ngai, *Phys. Rev. Lett.* 86 (2001) 1279;  
A. Rivera, C. León, J. Sanz, J. Santamaria, C.T. Moynihan, K.L. Ngai, *Phys. Rev. Lett.*, in press.